Transition frequencies of the *D* lines of ^{39}K, ^{40}K, and ^{41}K measured with a femtosecond laser frequency comb

Stephan Falke, Eberhard Tiemann, and Christian Lisdat*
Institut für Quantenoptik, Universität Hannover, Welfengarten 1, 30167 Hannover, Germany

Harald Schnatz and Gesine Grosche
Physikalisch-Technische Bundesanstalt, Bundesallee 100, 38116 Braunschweig, Germany

(Received 11 May 2006; published 6 September 2006)

We report measurements of the transition frequencies $4s\ ^2S_{1/2}-4p\ ^2P_{1/2}$ and $4s\ ^2S_{1/2}-4p\ ^2P_{3/2}$ of the potassium isotopes 39, 40, and 41 through an atomic beam experiment with a fractional uncertainty of about 2×10^{-10}. For frequency calibration, a fs-laser comb referenced to a Cs atomic clock was used. Compared to previous results, hyperfine constants for the states $4p\ ^2P_{1/2}$ and $4p\ ^2P_{3/2}$ and isotope shifts are given with a considerably reduced uncertainty. This paper also resolves the discrepancy of transition frequencies measured by Banerjee *et al.* [Phys. Rev. A **70**, 052505 (2004)] and Scherf *et al.* [Z. Phys. D **36**, 31 (1996)] and the hyperfine constant $A(^{39}\mathrm{K}, ^2P_{1/2})$ reported by Banerjee *et al.* [Europhys. Lett. **65**, 172 (2004)] and Bendali *et al.* [J. Phys. B **14**, 4231 (1981)].

DOI: 10.1103/PhysRevA.74.032503 PACS number(s): 32.30.−r, 32.10.Fn, 42.62.Fi, 06.30.Ft

I. INTRODUCTION

The advent of femtosecond laser frequency combs has greatly simplified precision experiments in optical spectroscopy [1]. Of high importance are experiments which test fundamental concepts in physics, e.g., the time independence of constants like the fine structure constant α. Here, the precise knowledge of optical transition frequencies of different atoms or molecules can be exploited to deduce variations of α [2]. Precise spectroscopic information also allows to test atomic structure calculations and can be used to determine properties of the nucleus like the nuclear moment or effective charge radius. Furthermore, well-known transition frequencies can serve efficiently as frequency references for other experiments. Very successful experiments have been performed with various atoms [3,4] and in particular with alkali-metal atoms [5–8]. For potassium, Banerjee *et al.* recently investigated the most abundant isotope ^{39}K by saturation spectroscopy [9–11]. For these measurements, either a Michelson interferometer or a transfer cavity with known free spectral range was used [12]. One determines the difference frequency between a known laser (typically locked to the D_2 line of ^{85}Rb) and the laser used for spectroscopy on the system of interest. Banerjee *et al.* showed that their results agree with published ones from 1956 [13], but did not discuss more recently measured transition frequencies with improved uncertainty with respect to Ref. [13], that deviate more than 400 MHz from their results [14]. A similar discrepancy exists for the magnetic dipole coupling constant $A(^{39}\mathrm{K})$ of the $4p\ ^2P_{1/2}$ state reported in Ref. [11], which agrees with the value from Ref. [15], but is inconsistent with values in Refs. [16,17]. A more detailed discussion of these points will be given in Sec. IV A in combination with our own preinvestigations.

To resolve these discrepancies, we have now carried out precision measurements of the *D* lines of potassium with an improved experimental setup. For the frequency measurement, we use a fs-laser frequency comb referenced to a portable Cs atomic clock with an uncertainty below 10^{-11}. We have probed the potassium atoms in a highly collimated atomic beam. This method has the advantage over cell experiments that the Doppler width can be reduced well below the natural linewidth. The absence of a broad Doppler background allows the observation of the less abundant isotopes ^{40}K and ^{41}K [16]. Special care must be taken, as this experimental technique suffers from possible systematic shifts caused by a Doppler shift due to misalignment of laser probe beam and atomic beam. However, it has been shown that this drawback can be overcome by thorough adjustment with the help of a retroreflector [6] or by reciprocal fiber coupling [18].

II. EXPERIMENTAL SETUP

The atomic beam apparatus has been described previously in Ref. [19]. The beam has supersonic character though no carrier gas is used. The mean particle velocity is about 1000 m/s with a velocity spread of ±100 m/s. The beam has a collimation ratio of about 1000, which leads to a residual Doppler width of approximately 2 MHz in the spectral region considered here. The residual gas pressure in the interaction zone is below 10^{-8} mbar and the density of atoms in the beam is of the order of 10^9 cm^{-3}. The solid angle of detection is about 1.4 sr, the fluorescence is detected by a photomultiplier and current amplifier. The interaction volume of atomic and laser beam is shielded from magnetic fields by a μ-metal box, which reduces the residual magnetic field to below 20 mG.

Figure 1 shows schematically the optical setup. Light from an extended-cavity diode laser in Littrow configuration (called spectroscopy laser) is transferred with an optical fiber from a quiet laboratory to the atomic beam apparatus. The atoms are probed with a linearly polarized laser beam of 2 mm diameter. The polarization axis with respect to the

*Electronic address: lisdat@iqo.uni-hannover.de

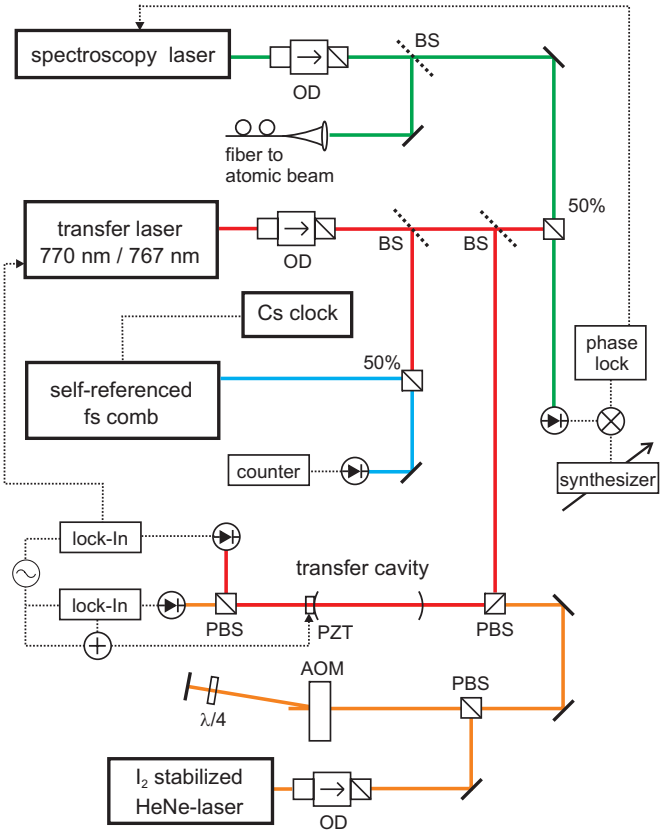

FIG. 1. (Color online) Laser system used for the frequency measurement. OD, optical diode; BS, beam splitter; 50%, 50% beam splitter; PBS, polarizing beam splitter; PZT, piezoelectric actuator; λ/4, λ/4 retarder.

residual magnetic field is unknown and possible errors are included in our analysis. The spectroscopy laser is locked to a cw titanium-sapphire transfer laser by stabilizing the beat note of both with a phase-frequency comperator. Its reference frequency is provided by a frequency synthesizer, which is controlled by the data acquisition system.

The frequency of the transfer laser is determined with a self-referenced Ti:sapphire fs-laser frequency comb by counting the beat note between the transfer laser and a comb tooth of the fs comb. The repetition of the fs comb (about 700 MHz) is stabilized using the clock signal of a commercial Cs clock. The counted frequency value is used for the determination of the transfer laser frequency. The carrier-envelope-offset frequency ν_{ceo} of the frequency comb is not stabilized but counted. All counters have a gate time of 1 s.

To improve the frequency stability of the transfer laser, it is stabilized via a tunable transfer cavity to an I_2 stabilized He:Ne laser. Arbitrary difference frequencies are accessible by an acousto-optical modulator (AOM). In this way we observe a fractional frequency stability of the transfer laser of $3\times10^{-11}\tau^{-1/2}$, where τ is the averaging time in seconds. The frequency comb generator in connection with the Cs clock allows to measure its frequency with a fractional accuracy of about 10^{-11} in 1 s.

To record the potassium spectra, the diode laser is tuned by the data acquisition system via the synthesizer as shown in Fig. 1, while the frequency of the transfer laser is counted by the fs comb. The synchronization between both recordings is done by additionally counting the synthesizer frequency. The typical step size of the spectroscopy laser was 200 kHz, the recording time per point 200 ms with 20 ms dead time to allow for delays in the frequency settling of the synthesizer. We recorded both directions of scan to detect and reduce shifts from electronic time constants.

III. DOPPLER COMPENSATION

In precision experiments with particle beams, it is important to minimize the residual first order Doppler shift. It appears if the angle between probe laser beam and atomic beam deviates from 90°. For this purpose, we have recorded our spectra utilizing a cat's eye. It ideally retroreflects the probe laser beam in itself without losses through the interaction region with the atomic beam. The retroreflector consists out of an achromatic lens with 30 cm focal length and mirror in a gimbal mount. The distance between mirror and lens must be exactly the focal length of the lens to achieve antiparallelism of incoming and outgoing beam. It can be set by a micrometer screw adjustable translation stage, the alignment was done by means of an optical interferometer in which the cat's eye served as one end mirror.

According to Ref. [20], the residual angle between both beams can be inferred from the uncertainty of the mirror's position, the residual angle between the axis of the cat's eye and the laser beam and the spatial displacement of the laser beam from the axis. Under our conditions we estimate a residual angle of less than 10 μrad between incoming and outgoing beam.

Assuming similar excitation and detection efficiency for both laser beam directions, the observed fluorescence signal will be symmetric around the unshifted frequency. Any deviation of the one-beam frequency from this Doppler-shift-free frequency can be due to either a residual Doppler shift or asymmetry. The residuals scatter after fitting a single beam profile with a symmetric model function justifies that for a Doppler shift smaller than the residual Doppler width, the measured profile is sufficiently symmetric. Thus, the deviation must be accounted to the residual Doppler shift in the single beam measurement and the resulting frequency of the two beam experiment can be considered Doppler-shift free.

If the signals from both beam directions do not have the same strength, the observed line will not be centered at the Doppler free frequency. The imperfection of the Doppler compensation can be estimated from the intensity of one- and two-beam spectra. The deviation from the optimum factor of 2 between both spectra was less than 25%, from which a remaining error from the Doppler effect of less than 50 kHz can be inferred with the help of line profile simulations. Here, the imperfection of the cat's eye is already included.

We confirmed these considerations by a measurement with a completely independent technique. Two antiparallel laser beams of the same intensity were generated by utilizing laser beams from two optical fibers and coupling the beam of one fiber into the other. With this technique a remaining angle between both beams of below 35 μrad can be achieved

[18], this limit corresponds to a shift of about 50 kHz. Spectra with both fibers were recorded independently, the averaged frequency is considered Doppler free. We have reproduced the measured frequency from one side within 10 kHz after recoupling that fiber, but will not claim to be in general better than the estimated 50 kHz. The average from both directions deviated for several lines by less than 30 kHz from transition frequencies measured with the cat's eye technique. Our final measurements were performed with the cat's eye technique because of a better long-term stability.

Moreover, from measurements with and without cat's eye one could derive the sign of the remaining Doppler shift with retroreflector. In combination with the estimated Doppler suppression, a frequency correction can be calculated, which corresponded in sign and magnitude to the observed difference between measurements with two fibers and cat's eye. However, the correction of the remaining uncompensated Doppler shift is much smaller than its uncertainty. Therefore, no correction was applied.

IV. MEASUREMENTS AND ANALYSIS

A. Frequency preinvestigations

We have outlined in the introduction that inconsistent frequency values for the potassium *D* lines of ^{39}K appear in the literature. Banerjee *et al.* [10,11] reached an uncertainty of about 100 kHz for the D_2 line and better for the D_1 transitions. They compared their results with the value from Risberg [13]. Risberg's measurements had for the potassium *D* lines a rather large uncertainty of about 800 MHz plus uncertainties stemming from the dispersion correction formula [21] used to calculate vacuum wave numbers. The authors of Refs. [10,11] did not discuss the measurements of Scherf *et al.* [14]. Here, an uncertainty of 20 MHz is stated.

The discrepancy between Scherf and Banerjee is more than 400 MHz, which is not only many times the respective uncertainty but also comparatively easy to detect with classical spectroscopic means. Thus, we have performed several checks before the fs comb supported frequency measurement.

Potassium spectra were recorded together with I_2 Doppler broadened absorption spectra, that can be used as a frequency calibration with an uncertainty of about 100 MHz. The frequency of the nearest I_2 line was taken either from the iodine atlas [22] or from a simulation of the I_2 spectrum [23]. Both values are in perfect agreement. Furthermore, the frequency was measured with two commercial wavelength meters (HighFinesse WS-7, WS-8) with a reduced uncertainty of 100 MHz and 40 MHz, respectively. These methods have sufficient accuracy to distinguish between transition frequencies from both groups. All results were consistent with the transition frequencies given by Scherf [14].

Thus, we must conclude that possibly the starting value of Banerjee *et al.* was not sufficiently precise to unambiguously determine the *D* lines' frequencies. This is also a possible explanation for the deviation between their hyperfine parameters and the values given in Refs. [16,17].

B. D_1 line

All lines belonging to the D_1 line at 12 985 cm^{-1} of potassium are spectrally comparatively well isolated. They are grouped in pairs of two lines with common lower hyperfine level F and differing total angular momentum F' in the excited state. Thus two groups of two lines each were measured for the isotopes 39, 40, and 41. The spectra were recorded with retroreflector to compensate for Doppler shifts. The typical peak intensity per laser beam was 13 μW/cm^2 of ^{39,41}K, while 280 μW/cm^2 had to be used to achieve a reasonable signal-to-noise ratio for ^{40}K. The residual Doppler shift was regularly checked by recording spectra without cat's eye to exclude unnoticed drifts in the setup.

One record of the transition $F=2\rightarrow F'=1,2$ is shown in Fig. 2. Each line was fitted with a modified Lorentzian function, where the parameters for amplitude, linewidth, and center frequency ν_0 were independent for both hyperfine transitions. Additionally, a constant background to account for stray laser light or photomultiplier dark current was adjusted. The Lorentzian profile was modified, since a small residual Doppler effect is expected. Due to the narrow velocity distribution of the atoms in the direction of flight and the high collimation ratio of the beam, we assumed constant amplitudes for the Doppler components in the frequency interval $\nu_0 \pm \nu_D$, and zero outside. The fitted values for ν_D were for all fits in good agreement with the expected value of about 1 MHz. The fitted homogeneous linewidth is about 6.5 MHz, which is very close to the value of 6.0 MHz expected from the lifetime of the excited state [25]. The residuals of the fit are depicted in the lower trace of Fig. 2. A very good description of the observed line profiles is achieved.

When spectra of the less abundant isotopes ^{40}K and ^{41}K were fitted, additionally a frequency dependent background had to be taken into account. It originates from the Lorentzian wings of the transitions in the main isotope ^{39}K. For the background, the same function as described above was used; but only its amplitude was a fitting parameter. The width was fixed to a typical value, while the center frequency was taken from the nearest hyperfine transition of ^{39}K. An example for the transition $F=9/2\rightarrow F'=9/2,7/2$ in ^{40}K is shown in Fig. 3. The residuals in the lower part of the figure are again very

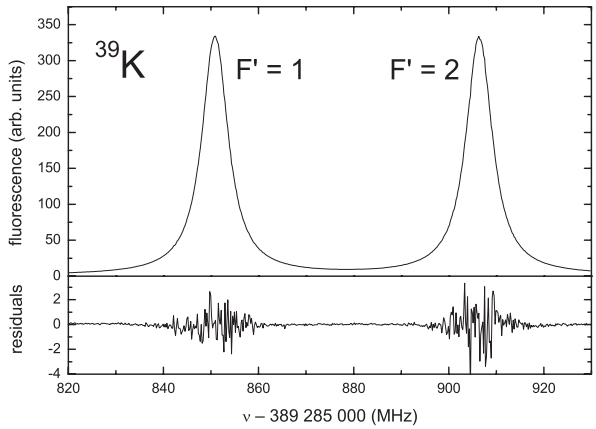

FIG. 2. Record of the D_1 transitions $F=2\rightarrow F'=1,2$ in ^{39}K. The lower trace shows the residuals of the fit, which was used to determine the line center. Note the zoom factor of about 50.

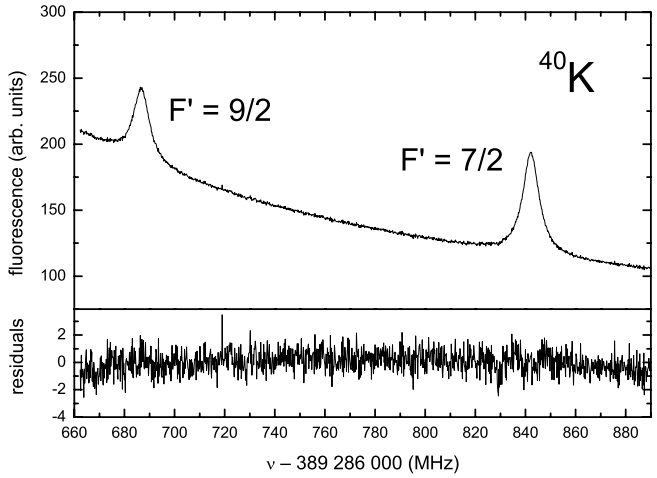

FIG. 3. The D_1 transitions $F=9/2\rightarrow F'=9/2,7/2$ in ^{40}K. The frequency dependent background stems from the wings of the transitions in ^{39}K. The lower trace shows the residuals of the fit magnified by a factor of about 40.

small and do not show any systematic deviations.

The statistical uncertainty of the fitted transition frequencies depend on the signal-to-noise ratio of the spectra. For the stronger spectra of ^{39,41}K, typically a value below 4 kHz was determined by the fit. For ^{40}K the statistical uncertainty is around 15 kHz.

A very significant consistency check of the data is to derive the ground state hyperfine splitting. We calculated it from the mean transition frequencies. Our values for the D_1 lines agree with the well-known microwave spectroscopy data (Ref. [26] ^{39}K, 461.720 MHz; ^{40}K, −1285.79 MHz; and ^{41}K, 254.014 MHz; values rounded to digits needed in the present case) to within 20 kHz. The hyperfine splittings of the excited state measured from ground states with different F are consistent within 10 kHz, which is another verification.

Deviations of this magnitude are consistent with imperfections and changes in the Doppler compensation (Sec. III) or other systematic line shifts (see Sec. IV D), but can also be attributed to a larger error in the determination of the line center and underestimation of the corresponding uncertainty by the fit. An interpretation along this line is indicated by the increased deviation of the likewise determined ground state splitting in ^{40}K of 38 kHz for the common upper level $F'=9/2$ and even 140 kHz for $F'=7/2$, respectively. It must be noticed that the transition $F=7/2\rightarrow F'=7/2$ is very weak and sitting on a comparatively steep background. An exceptionally large variation in the residual Doppler effect due to rapid changes in the optical alignment can be excluded since the transition $F=7/2\rightarrow F'=9/2$ was recorded in the same scan. The statistical uncertainty of the $F=7/2\rightarrow F'=7/2$ line's frequency is with 35 kHz more than 2 times as big as for the other transitions of ^{40}K. We conclude therefore that the uncertainty in the determination of the line center is underestimated by the fit. Realistic uncertainty contributions for the determination of the line center are 20 kHz and 40 kHz for ^{39,41}K and ^{40}K, respectively.

C. D_2 line

The D_2 lines of potassium at 13 042 cm^{-1} were measured in a similar way to the D_1 lines. Differences in the analysis arise from the very small hyperfine splitting in the $^2P_{3/2}$ state of ^{39}K that leads to a triplet of transitions overlapping within the natural linewidth (see Fig. 4). The situation is even worse for ^{41}K (see Fig. 5), where the hyperfine splitting is about a factor of 2 smaller than in ^{39}K [27].

Besides the nuclear magnetic dipole interaction parametrized by the A factor, for the $^2P_{3/2}$ level the electric quadrupole interaction must be taken into account, which is represented by the coupling constant B. For the individual analysis of each hyperfine group, this leads to the difficult situation that three free parameters determining the line positions must be adjusted to an overlapping structure.

It was therefore preferred to perform joint fits of both groups' spectra $F=1$ and $F=2$ of each isotope with common hyperfine parameters. In this way, six transitions observed and recorded several times were described by only three parameters for the frequency, where we made use of the very precisely known ground state splitting $F=1\leftrightarrow F=2$ [26]. The other parameters discussed in Sec. IV B were individually adjusted for each recorded spectrum, but only two Lorentzian linewidths were fitted to further reduce the number of free parameters: we found that the transitions with $\Delta F=\pm 1$ are satisfactorily described with a common Lorentzian linewidth. All lines are modeled with the same Doppler width.

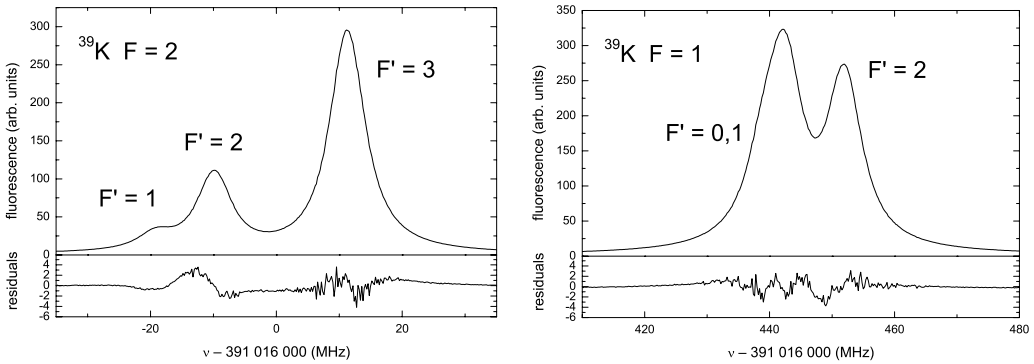

FIG. 4. Spectrum of the transitions belonging to the D_2 line of ^{39}K. On the left-hand side, the lower hyperfine state is $F=2$, the right-hand side depicts the spectrum from $F=1$. The residuals are enlarged by a factor 30.

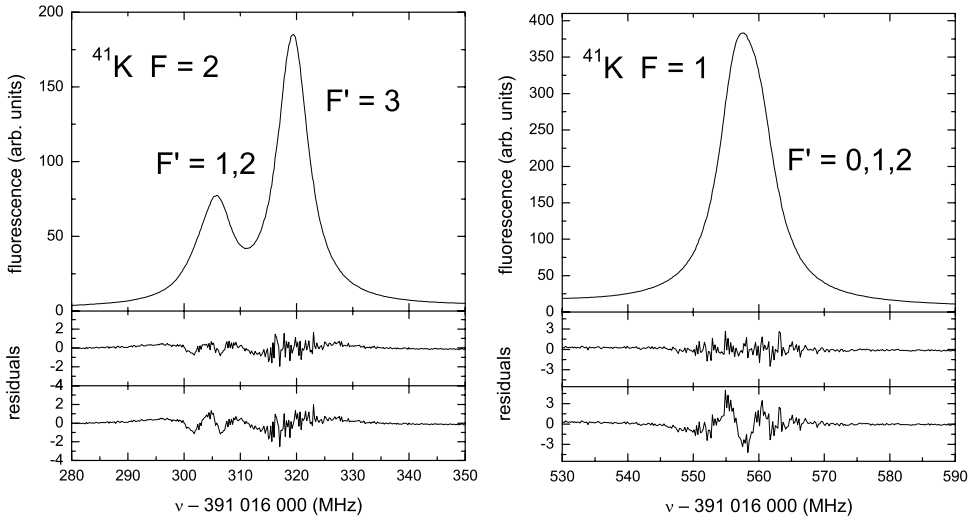

FIG. 5. The $F=2\rightarrow F'=1,2,3$ component of the ^{41}K D_2 line (left-hand side), and the spectrum of $F=1\rightarrow F'=0,1,2$ (right-hand side) is shown. In both parts, two curves with residuals are shown. The upper one is obtained when the hyperfine constants of the $^2P_{3/2}$ state are fitted. For the lower case, they were fixed to literature values [27] (see text).

With these restrictions, the fitting is much more deterministic and produces reliable results. Such a lengthy fitting procedure was not necessary in the case of the D_1 lines, where the transitions are well separated and frequencies can be evaluated easily for each line.

The consistency of the measurements was checked by the isotope ^{40}K, which has a larger hyperfine splitting and shows less overlapping line profiles. The expected ground state splitting is reproduced with a deviation of less than 40 kHz by fitting the center frequency of each hyperfine multiplet individually with common parameters A and B.

The residuals depicted in Fig. 4 for the ^{39}K D_2 line indicate some remaining mismatch of experimental observations and fit. This is also true but less severe in the case of ^{41}K (Fig. 5), while for ^{40}K the quality of the fit is comparable to the one shown in Fig. 3. In Fig. 5, two traces of residuals are depicted for each group. They stem from fits with freely adjusted hyperfine parameters of the $^2P_{3/2}$ state and from a fit, where they were fixed to the values from Ref. [27]. We will come to this again in Sec. V.

We attribute the deviations to weak effects of optical pumping. Attempts to fit our spectra with a density matrix approach using our experimental parameters lead to no significant improvement. This may be due to the fact that the polarization of the spectroscopy laser beam with respect to the residual magnetic field is not known. We are therefore forced to increase for ^{39}K and ^{41}K the uncertainty, with which we can determine the line center. An uncertainty of 100 kHz is in our opinion well justified.

D. Uncertainty budget

The precision of the performed measurements is limited by several effects. The most crucial one is the residual first order Doppler effect, which was already discussed in Sec. III. There, we showed that we can limit its influence to below 50 kHz for the absolute frequency. For relative frequency measurements, the contribution to the uncertainty budget from the Doppler shift will be smaller when the optical alignment is unchanged and not drifting. By repeated measurements with and without retroreflected beam we monitored the change of the Doppler shift in time and estimated that the uncertainty contribution for difference frequency measurements is 20 kHz for data taken within a few hours.

The second order Doppler effect cannot be avoided by the use of a retroreflector. For the most probable particle velocity of 1000 ± 100 m/s we have measured in our beam it amounts to $-2.2(5)$ kHz. The velocity of the atoms was determined by means of a Doppler detector [24]. We have corrected the transition frequencies for the second order Doppler effect.

Magnetic fields are shielded from the interaction region by a μ-metal box. The remaining field of less than 20 mG can lead to a line shift of less than 30 kHz.

Two systematic shifts occur due to the photon recoil. To begin with, the peak of the absorption profile of an atom at rest is shifted from transition frequency ν_0 corresponding to the energy difference of the two involved levels by the recoil energy $h\nu_r=h^2\upsilon_0^2/2M_{\mathrm{K}}c^2\approx 8.7$ kHz$\times h$ for the potassium D lines. Here, h is Planck's constant, c the speed of light, and M_{K} is the mass of the potassium atom.

The second contribution stems from the average velocity of $\upsilon_r=h(\nu_0+\nu_r)/M_{\mathrm{K}}c\approx 1.3\times10^{-2}$ m/s gained by the atom after an absorption-emission cycle. Multiple cycles lead to a velocity redistribution and thus Doppler shift and line asymmetry. The maximum Doppler shift $2\times\nu_r$ per cycle is about 17 kHz.

This influence can be kept small by low laser intensity and is further reduced by the two counter-propagating laser fields produced by the retroreflector. We have calculated that under our experimental conditions for a laser beam in only one direction, on average less than 0.2 photons are scattered per atom for ^{39,41}K and 3 for ^{40}K. We think that shifts due to velocity redistribution are smaller than 1 kHz for ^{39}K and for ^{41}K. These considerations are very well confirmed by the observed intensity ratio of the lines that matches the relative line strengths for unsaturated excitation better than 3% for clearly separated lines, for which the intensities can be well determined.

For ^{40}K systematic frequency shifts could be present due to the higher number of scattered photons. Since the difference of intensity in the counter-propagating beams of the cat's eye is less than 25% the Doppler shift will mostly can-

TABLE I. Summary of the different contributions to the error budget. The values in parentheses for the sum in quadrature refer to relative measurements with a reduced Doppler uncertainty.

Source	Correction	Uncertainty
First order Doppler effect	0 kHz	50 kHz
(for relative measurement)	(0 kHz)	(20 kHz)
Second order Doppler effect	2.2 kHz	0.5 kHz
Zeeman effect	0 kHz	30 kHz
Recoil shift	−8.7 kHz	0.1 kHz
Velocity redistribution		
^{39,41}K	0 kHz	1 kHz
^{40}K	0 kHz	15 kHz
ac-Stark effect		
D_2 line ^{40}K	0 kHz	50 kHz
All other lines	0 kHz	6 kHz
Line center/profile		
^{39,41}K D_1		20 kHz
^{39,41}K D_2		100 kHz
^{40}K		40 kHz
Frequency measurement	0 kHz	1 kHz
	Sum	Sum in quadrature
D_1 ^{39,41}K	−6.5 kHz	62(42) kHz
^{40}K	−6.5 kHz	73(56) kHz
D_2 ^{39,41}K	−6.5 kHz	116(107) kHz
^{40}K	−6.5 kHz	88(75) kHz

cel. We attribute an uncertainty of 15 kHz to the possibly remaining asymmetry, which corresponds to difference of 1.5 in the number of scattered photons for both laser beam directions. A significant influence of optical pumping is observed for ^{40}K only on the cycling transition $F=9/2 \leftrightarrow F'=11/2$ of the D_2 line. For the other transitions, the expected and observed intensity ratios match within 7%. An energetic shift of the levels due to, e.g., the Zeeman or ac-Stark effect and optical pumping could lead to additional line shifts. Since the uncertainties for Zeeman and Stark shifts discussed below account for the maximum expected effect, no additional uncertainty contribution appears here.

Coupling of the spectroscopy laser beam to near resonant transitions, in particular within the hyperfine multiplet, leads to an ac-Stark shift of the resonant transition. The shift can become important when the energetic spacing between transitions with common levels is small. This is the case for the small hyperfine splitting of potassium, especially in the $^2P_{3/2}$ state.

The maximum possible ac-Stark shift can be calculated with sufficient accuracy making use of the lifetime of the $4p\ ^2P$ levels to determine the transition dipole moment. One of the most precise methods to determine the lifetime of the first exited P levels in alkali metals is to calculate it from the resonant dipole-dipole coupling coefficient C_3, which is determined from spectroscopy of long range molecular states [25]. Note, that this calculation involves the knowledge of the transition frequency of the D lines, but the change of this value for ^{39}K does not influence the results of Ref. [25] significantly.

TABLE II. Transition frequencies ν of the D_1 lines. For convenience, an offset of 389 285 GHz is subtracted.

Isotope	F	F'	ν in MHz
^{39}K	1	1	1312.574(62)
	1	2	1368.124(62)
	2	1	850.838(62)
	2	2	906.386(62)
^{40}K	9/2	9/2	1686.785(73)
	9/2	7/2	1842.157(73)
	7/2	9/2	400.957(73)
	7/2	7/2	556.224(200)[a]
^{41}K	1	1	1433.888(62)
	1	2	1464.386(62)
	2	1	1179.890(62)
	2	2	1210.380(62)

[a]The larger uncertainty is due to the difficulties determining the line center discussed in Sec. IV B.

The ac-Stark shift due to nonresonant coupling of the spectroscopy laser field is given for sufficiently large detunings Δ (here, Δ larger than the natural linewidth) by the eigenenergies of a two level system in the dressed state picture

$$\frac{1}{2}(\Delta \pm \sqrt{\Delta^2 + \Omega^2}), \tag{1}$$

where $2\pi\Omega$ is the Rabi frequency. For determining an upper limit of the ac-Stark effect we calculate with twice the peak intensity of a single beam to account for the retroreflected beam. The detuning Δ must be set to the hyperfine splitting of the excited state. The hyperfine splitting of the ground state is large enough, such that coupling to the other ground state hyperfine state can be neglected. For the D_1 line, ac-Stark shifts are below 6 kHz for all isotopes. The larger hyperfine splitting of ^{40}K compensates for the higher intensity that was necessary to observe this isotope.

The hyperfine splittings of the $^2P_{3/2}$ state are smaller than for $^2P_{1/2}$. Due to the overlap of lines, a simple calculation according to Eq. (1) strongly overestimates the possible Stark shifts of the D_2 lines. In order to derive a more realistic limit, we undertook density matrix simulations modeling the experimental conditions. From these calculations, we derive an upper limit of 6 kHz for ^{39}K and ^{41}K and 50 kHz for ^{40}K.

The last contribution to the uncertainty budget stems from the frequency measurement itself. It amounts to less than 1 kHz for the synchronization of the frequency trace and spectrum and the uncertainty of the Cs clock.

In Table I, we have summarized the contributions to the uncertainty budget of the transition frequency.

TABLE III. Derived hyperfine parameters A and B and constants from literature. All values are in MHz.

Isotope	Source	$A\,^2P_{1/2}$	$A\,^2P_{3/2}$	$B\,^2P_{3/2}$
^{39}K	This work	27.775(42)	6.093(25)	2.786(71)
	Ref. [16]	27.80(15)		
	Ref. [17]	27.5(4)		
	Ref. [11]	28.859(15)		
	Ref. [15]	28.85(30)		
	Ref. [28]		6.00(10)	2.9(2)
	Ref. [29]		6.13(5)	2.72(12)
	Ref. [26]		6.06(8)	2.83(13)
^{40}K	This work	−34.523(25)	−7.585(10)	−3.445(90)
	Ref. [16]	−34.49(11)	−7.48(6)	−3.23(50)
	Ref. [30]		−7.59(6)	−3.5(5)
^{41}K	This work	15.245(42)	3.363(25)	3.351(71)
	Ref. [16]	15.19(21)		
	Ref. [17]	15.1(8)		
	Ref. [29]		3.40(8)	3.34(24)
	Ref. [27]		3.325(15)	3.320(23)

V. RESULTS

From the description of the measurements and analysis in Sec. IV it follows that we have determined the transition frequency of each hyperfine transition of the D_1 lines individually. The average values are given in Table II with the uncertainties and corrections according to Table I.

Using the transition frequencies in Table II, we have determined the hyperfine parameter A for all observed isotopes. Since the A factor depends on difference frequencies only, the reduced uncertainty stated in Table I can be applied. As uncertainty of the energy splitting of the excited levels we took twice this uncertainty. The A factor is connected to the level splitting by $\Delta\nu = A\cdot(F'+1)$ where F' is the smaller one of both quantum numbers involved in the excited state. Thus the uncertainty of the A factor is given by the uncertainty of the level splitting divided by $F'+1$.

TABLE IV. Hyperfine-free transition frequencies ν of the D_1 and D_2 lines.

Isotope	Source	$\nu(D_1)$ in MHz	$\nu(D_2)$ in MHz
^{39}K	fs comb	389 286 058.716(62)	391 016 170.03(12)
	Wavelength meter	389 286 068(40)	391 016 190(40)
	I_2	389 285 980(100)	
	[14]	389 286 078(20)	391 016 188(20)
	[10,11]	389 285 580.908(50)	391 015 578.04(11)
^{40}K	This work	389 286 184.353(73)	391 016 296.050(88)
^{41}K	This work	389 286 294.205(62)	391 016 406.21(12)

The values of the hyperfine parameters A are given in Table III and compared with literature values. All parameters are visualized in Fig. 6. It can be seen that the agreement of our A factor for the $^2P_{1/2}$ level and the results from Refs. [16,17] is very good while the values from Refs. [11,15] deviate from our results. In the case of Ref. [11], the deviation has possibly the same reasons as for the disagreement of the transition frequencies discussed in Sec. IV A. The transition frequencies and hyperfine parameters of both states can be combined to calculate hyperfine-free transition frequencies of each isotope's D_1 line. The values are given in Table IV. The results of the frequency comb measurements agree with our preinvestigations (see Sec. III) and Scherf's finding [14].

The analysis of the D_2 line data was done in a different way than in the case of the D_1 transition (see Sec. IV). The results of the fitting procedure are directly hyperfine-free transition frequencies and the hyperfine parameters of the $^2P_{3/2}$ level. Their uncertainties were determined from a fitting procedure, in which an artificial dataset with the reduced uncertainties given in Table I was used. The hyperfine-free transition frequencies are listed in Table IV, the hyperfine parameters are given in Table III and are depicted in Fig. 6. In Table V, we have given frequencies of comparatively weakly overlapping transitions of the D_2 line. They were calculated from the fitting procedure introduced in Sec. IV C.

The values of the hyperfine parameters are generally in agreement with previous measurements with the exception of

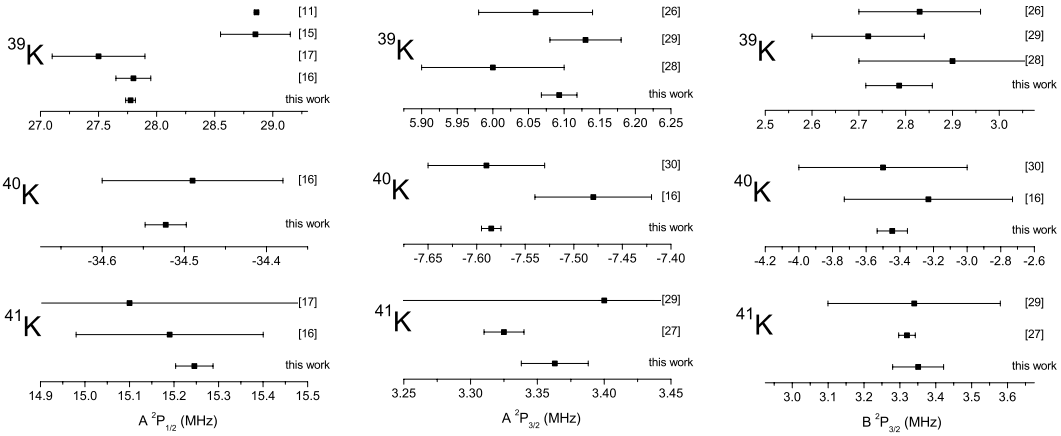

FIG. 6. Hyperfine constants determined from our work and by other authors. Left-hand side, $A\,^2P_{1/2}$; center, $A\,^2P_{3/2}$; right-hand side, $B\,^2P_{3/2}$.

TABLE V. Frequencies ν of weakly overlapping transitions of the D_2 lines. For convenience, an offset of 391 015 GHz is subtracted.

Isotope	F	F'	ν in MHz
^{39}K	2	3	1011.286(116)
^{40}K	9/2	11/2	1821.134(88)
	9/2	9/2	1865.221(88)
	9/2	7/2	1898.523(88)
	7/2	9/2	579.431(88)
	7/2	7/2	612.733(88)
	7/2	5/2	636.912(88)
^{41}K	2	3	1319.356(116)

$A(^{39}\mathrm{K}\ ^2P_{1/2})$, where we find the already discussed discrepancies. In the case of ^{41}K, where high precision measurements on the D_2 line were presented in Ref. [27], our results have a larger uncertainty than earlier measurements. We have shown in Fig. 5 that an acceptable fit of our spectra can be achieved with the parameters of Ref. [27], but the fit improves significantly by small variations of the hyperfine parameters. Thus, we give our fit results including the A and B parameters, also because of the completely different nature of both experiments.

From the hyperfine-free transition frequencies, the fine structure splitting and isotope shifts can be calculated. As reference isotope, we choose ^{39}K. We regard the measurements on different isotopes and D lines as sufficiently independent to add their uncertainties in quadrature. The results are given together with data from literature in Table VI. Our results are again consistent with the values from other sources with the exception of the value for the fine structure splitting given by Banerjee *et al.* [10].

VI. CONCLUSION

We have measured all optical transitions of both D lines in the isotopes 39, 40, and 41 of potassium by laser induced fluorescence spectroscopy on a highly collimated atomic beam with a fractional uncertainty of about 2×10^{-10}. The absolute frequencies were measured with a self-referenced femtosecond laser frequency comb generator that supplied the link from the spectroscopy laser to a Cs atomic clock.

TABLE VI. Isotope shifts (IS) and fine structure (FS) splittings for the observed isotopes. All units are MHz.

Isotope	Source	FS	IS(D_1)	IS(D_2)
^{39}K	This work	1 730 111.31(13)		
	[14]	1 730 110(30)		
	[10]	1 729 997.132(120)		
^{40}K	This work	1 730 111.70(12)	125.64(10)	126.03(15)
	[16]		125.58(26)	126.43(30)
^{41}K	This work	1 730 112.01(13)	235.49(9)	236.18(17)
	[16]		235.27(33)	236.15(37)
	[17]		235.25(75)	

With our measurements, we confirm the transition frequencies for ^{39}K measured by Scherf *et al.* [14] or determined by conventional spectroscopic means like the I_2 atlas or commercial wavelength meters. We were not able to reproduce the results of Refs. [9–11].

From our measurements, the fine structure interval and hyperfine parameters A and B for the excited states $4p\ ^2P_{1/2}$ and $4p\ ^2P_{3/2}$ were derived. They have a significantly reduced uncertainty compared to data from literature and are consistent with those. The isotope shifts of D_1 and D_2 line of ^{40}K and ^{41}K were determined from the hyperfine-free transition frequencies with reduced uncertainty.

ACKNOWLEDGMENTS

The authors would like to thank Andreas Bauch from the PTB time division for providing the atomic clock and Ivan Sherstov for the construction of the μ-metal box. This project was accomplished within the Sonderforschungsbereich SFB 407 supported by the Deutsche Forschungsgemeinschaft (DFG).

[1] J. Ye, H. Schnatz, and L. Hollberg, IEEE J. Sel. Top. Quantum Electron. **9**, 1041 (2003).
[2] E. Peik, B. Lipphardt, H. Schnatz, T. Schneider, Ch. Tamm, and S. G. Karshenboim, Phys. Rev. Lett. **93**, 170801 (2004).
[3] T. J. Quinn, Metrologia **40**, 103 (2003), and references therein.
[4] D. Das, S. Barthwal, A. Banerjee, and V. Natarajan, Phys. Rev. A **72**, 032506 (2005).
[5] V. Gerginov, A. Derevianko, and C. E. Tanner, Phys. Rev. Lett. **91**, 072501 (2003).
[6] V. Gerginov, C. E. Tanner, S. Diddams, A. Bartels, and L. Hollberg, Phys. Rev. A **70**, 042505 (2004).
[7] J. Ye, S. Schwartz, P. Junger, and J. L. Hall, Opt. Lett. **21**, 1280 (1996).
[8] G. P. Barwood, P. Gill, and W. R. C. Rowley, Appl. Phys. B: Laser Opt. **53**, 142 (1991).
[9] A. Banerjee, D. Das, and V. Natarajan, J. Opt. Soc. Am. B **21**, 79 (2004).
[10] A. Banerjee and V. Natarajan, Phys. Rev. A **70**, 052505 (2004).
[11] A. Banerjee, D. Das, and V. Natarajan, Europhys. Lett. **65**, 172 (2004).
[12] A. Banerjee, D. Das, and V. Natarajan, Opt. Lett. **28**, 1579 (2003).
[13] P. Risberg, Ark. Fys. **10**, 583 (1956).
[14] W. Scherf, O. Kait, H. Jäger, and L. Windholz, Z. Phys. D: At., Mol. Clusters **36**, 31 (1996).
[15] P. Buck and I. Rabi, Phys. Rev. **107**, 1291 (1957).
[16] N. Bendali, H. T. Duong, and J. L. Vialle, J. Phys. B **14**, 4231

(1981).
[17] F. Touchard, P. Guimbal, S. Büttgenbach, R. Klapisch, M. De Saint Simon, J. M. Serre, C. Thibault, H. T. Duong, P. Juncar, S. Liberman, J. Pinard, and J. L. Vialle, Phys. Lett. **108B**, 169 (1982).
[18] G. Wilpers, C. Degenhardt, T. Binnewies, A. Chernyshov, F. Riehle, J. Helmcke, and U. Sterr, Appl. Phys. B: Lasers Opt. **76**, 149 (2003).
[19] Ch. Lisdat, O. Dulieu, H. Knöckel, and E. Tiemann, Eur. Phys. J. D **17**, 319 (2001).
[20] K. Sengstock, Dissertation, Universität Bonn, available at http://www.ulb.uni-bonn.de/webOPAC/
[21] B. Edlén, J. Opt. Soc. Am. **43**, 339 (1953).
[22] S. Gerstenkorn, J. Vergés, and J. Chevillard, *Atlas du Spectre de l'Absorption de la Molécule D'iode [11000–14000 cm^{-1}]* (Laboratoire Aimé Cotton, CNRS II, Orsay, France, 1982).
[23] H. Knöckel, B. Bodermann, and E. Tiemann, Eur. Phys. J. D **28**, 199 (2004).
[24] U. Hefter and K. Bergmann, in *Atomic and Molecular Beam Methods*, edited by G. Scoles (Oxford University Press, Oxford, 1988), Vol. I.
[25] H. Wang, P. L. Gould, and W. C. Stwalley, J. Chem. Phys. **106**, 7899 (1997).
[26] E. Arimondo, M. Inguscio, and P. Violino, Rev. Mod. Phys. **49**, 31 (1977).
[27] A. Sieradzan, P. Kulatunga, and M. Havey, Phys. Rev. A **52**, 4447 (1995).
[28] R. W. Schmieder, A. Lurio, and W. Harper, Phys. Rev. **173**, 76 (1968).
[29] J. Ney, Z. Phys. **223**, 126 (1969).
[30] J. Ney, R. Repnow, H. Bucke, and G. Schatz, Z. Phys. **213**, 192 (1968).